21 May 2007
Volume 90 Number 21

APPLIED PHYSICS LETTERS

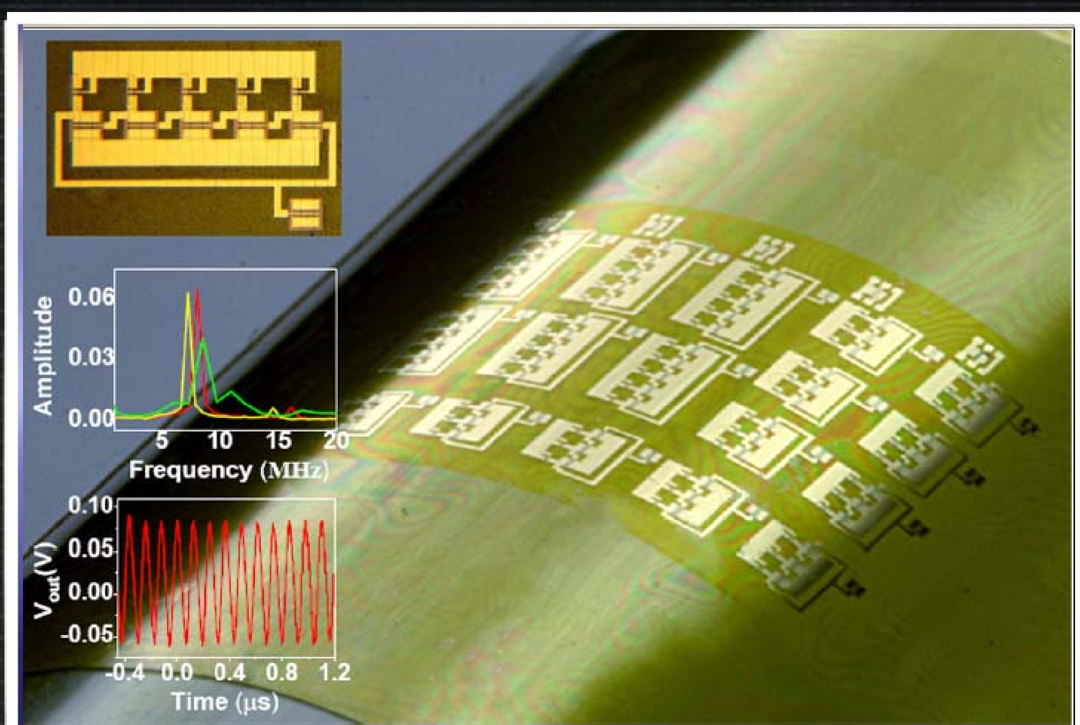

0003-6951(20030224)82:8;1-7

Available online–
See http://ojps.aip.org/aplo/
AMERICAN INSTITUTE OF PHYSICS

Bendable integrated circuits on plastic substrates by use of printed ribbons of single-crystalline silicon

Jong-Hyun Ahn, Hoon-Sik Kim, Etienne Menard, Keon Jae Lee, Zhengtao Zhu,[a)]
Dae-Hyeong Kim, Ralph G. Nuzzo, and John A. Rogers[b)]
Department of Materials Science and Engineering, Frederick Seitz Materials Research Laboratory and Beckman Institute for Advanced Science and Technology, Department of Chemistry, University of Illinois at Urbana-Champaign, Urbana, Illinois 61801

Islamshah Amlani, Vadim Kushner, and Shawn G. Thomas
Embedded Systems and Physical Sciences Laboratory, Motorola Inc., Tempe, Arizona 85284

Terrisa Duenas
Nextgen Aeronautics, Inc., Torrance, California 90505

(Received 1 March 2007; accepted 4 April 2007; published online 21 May 2007)

This letter presents studies of several simple integrated circuits—*n*-channel metal-oxide semiconductor inverters, five-stage ring oscillators, and differential amplifiers—formed on thin, bendable plastic substrates with printed ribbons of ultrathin single-crystalline silicon as the semiconductor. The inverters exhibit gains as high as 2.5, the ring oscillators operate with oscillation frequencies between 8 and 9 MHz at low supply voltages (~4 V), and the differential amplifiers show good performance and voltage gains of 1.3 for 500 mV input signals. The responses of these systems to bending-induced strains show that relatively moderate changes of individual transistors can be significant for the operation of circuits that incorporate many transistors. © *2007 American Institute of Physics*. [DOI: 10.1063/1.2742294]

Large area, mechanically flexible electronics could enable innovative classes of devices for information display, medical diagnostics, X-ray imagers, and other systems. Such applications require high performance and robust technologies for the circuits. A variety of semiconductor materials have been explored, ranging from amorphous silicon, to small molecule organics and polymers, to polycrystalline silicon, and other inorganics, to carbon nanotubes.[1–5] An alternative approach uses ribbons, wires, platelets, and other structural forms of single-crystalline inorganic semiconductors.[6,7] We and others have recently demonstrated this strategy by building a variety of devices including high performance *n*-channel metal-oxide semiconductor field effect transistors (NMOSFETs) that use single-crystalline silicon ribbons and membranes with submicron thicknesses, which we refer to as microstructured silicon.[8,9] This letter presents circuits that incorporate multiple transistors of this type, including *n*-channel metal-oxide semiconductor (NMOS) inverters (logic gates), five-stage ring oscillators, and differential amplifiers, all supported on thin, flexible plastic sheets. Studies of the changes in electrical properties caused by mechanical bending reveal variations that, although small on an individual device basis, can be significant for operation of the circuits. These results could represent important considerations for the design of flexible electronic systems.

The fabrication of the devices presented here began with the formation of contact doped regions in the top layer of a silicon-on-insulator wafer (Soitec unibond with a 290 nm thick top Si layer and a 400 nm thick buried oxide layer).[8] For cost sensitive applications, related approaches that exploit commodity bulk wafers can be used.[10] Photolithography and etching processes defined ribbons from the top silicon layer; printing techniques delivered these ribbons in organized arrays to device substrates consisting of polyimide (PI) sheets (25 μm) coated with thin adhesive layers (~1.0 μm) of liquid PI precursor (polyamic acid, Sigma-Aldrich Inc.). Layers of SiO_2 (100 nm) formed by plasma-enhanced chemical vapor deposition served as the gate dielectrics. Etching through these layers and then defining metal patterns (Cr/Au, 5 nm/100 nm) by photolithography and lift-off created the source, drain, and gate electrodes for the transistors as well as the device interconnects needed to form circuits. Details of these processing procedures have been described elsewhere.[7,8]

Figure 1(a) shows representative current-voltage characteristics of an NMOSFET that has a channel length (L_c) of 2 μm, contact overlap (L_o) of 1.5 μm, and channel width (W) of 200 μm. The effective device mobilities, calculated using standard MOS model,[7] are ~550 and ~450 $cm^2/V\,s$ in the linear and saturation regimes, respectively. The on/off ratio is ~10^5, with a threshold voltage of ~0.1 V. The maximum gate-swing hysteresis, for the voltage ranges used here, is ~0.5 V, which we believe is likely caused by some amount of charge trapped in the SiO_2 and/or by defects associated with oxygen deficiencies at the interface between the Si and SiO_2 layer.[11] This moderate level of hysteresis does not represent a fundamental limit; it can be reduced further by appropriate choice of adhesive layer for the transfer and design of silicon ribbon structures. Devices of this type can operate at high frequencies. Figure 1(b) shows the cutoff frequency f_T as a function of drain current, determined without de-embedding parasitic capacitance of the pad fixture. The maximum f_T, measured at a gate/source voltage

[a)]Present address: Department of Chemistry, South Dakota School of Mines and Technology.

[b)]Author to whom correspondence should be addressed; electronic mail: jrogers@uiuc.edu

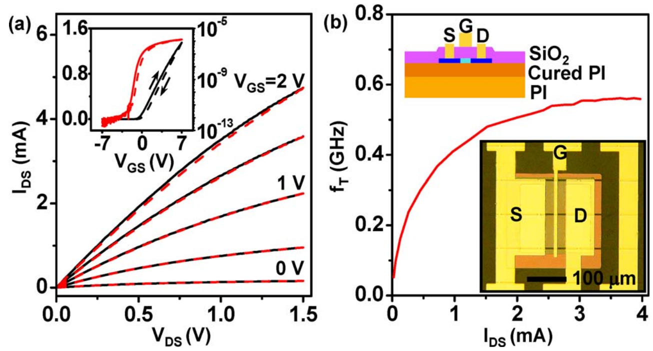

FIG. 1. (Color online) (a) Current-voltage characteristics of a representative device with a channel length, channel overlap distance, and channel width of L_c=2 μm, L_o=1.5 μm, and W=200 μm, respectively. The inset shows linear and log scale plots of transfer curves collected at V_{DD}=0.1 V. The devices show some modest amount of hysteresis (clockwise). (b) The cutoff frequency f_T as a function of I_{DS}. The insets show a schematic of cross section (top) and optical image of device (bottom).

V_{GS} of 2 V and a drain/source voltage V_{DS} of 1 V, is 570 MHz.

Transistors such as these can be integrated into circuits using similar types of processing techniques. An NMOS inverter represents one of the simplest examples. Figure 2 shows optical images, schematic illustrations, and electrical measurements of an NMOS inverter. The load and drive devices have channel widths of 30 and 200 μm, respectively. The values for L_c and L_o in both cases are 4 and 2.5 μm, respectively. These inverters exhibit well-defined transfer characteristics with gains of ~2.5 at a supply voltage of 3 V. The changes in electrical properties induced by bending were systematically evaluated using automated bending stages. Figure 2(b) shows a series of transfer curves obtained at different bending radii, corresponding to strains, estimated from the bend radii, of up to +0.23 and −0.23%. Although the inflection points in these curves moved slightly to the right after the first bending cycle, they remained stable and

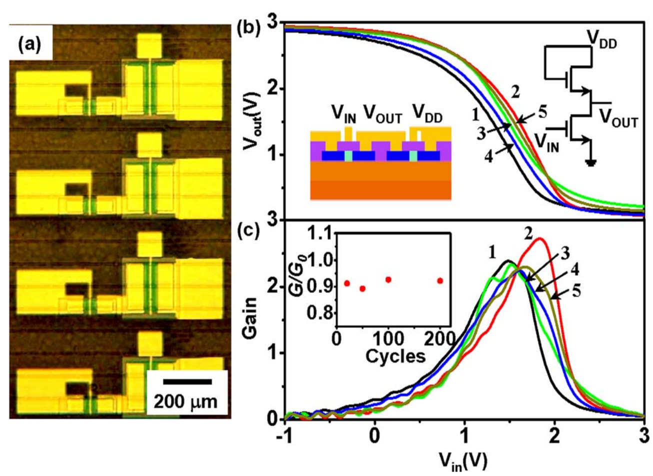

FIG. 2. (Color online) (a) Image of a printed array of NMOS inverters on a PI substrate. (b) Current-voltage characteristics of an inverter consisting of transistors of channel lengths L_c=5 μm and load-to-driver width ratio of 6.7, with W_{driver}=200 μm, with a 3 V supply at different bending radii [1-black: original state, 2-red: tension (0.16%), 3-green: tension (0.23%), 4-blue: compression (0.16%), and 5-dark yellow: compression (0.23%)]. The inset shows a schematic illustration of the inverter (left) and a circuit diagram (right). (c) Gain characteristics evaluated from the curves in (b). The inset shows the normalized peak gain as a function of bending cycles (to 6 mm bending radius, corresponding to ~0.23% strain).

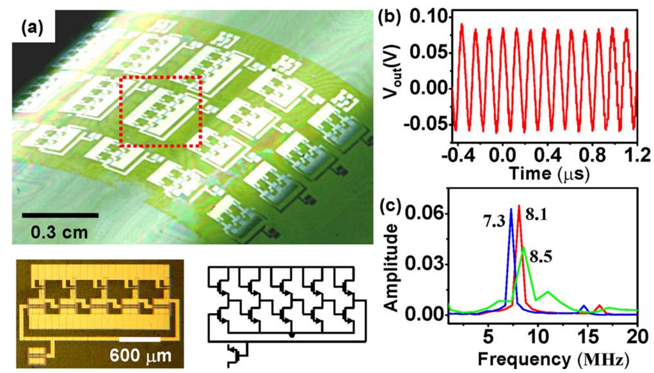

FIG. 3. (Color online) (a) Images of an array of five-stage ring oscillators on a PI substrate (top), magnified view of a single oscillator (bottom left) and circuit diagram (bottom right). (b) Output characteristics measured use a 4 V supply. (c) Fourier transform of time domain signals similar to the one in (b), collected at three different bending configurations. [red: unbent (8.1 MHz), green: 0.23% tension (8.5 MHz), and blue: 0.23% compression (7.3 MHz)].

reproducible in their response to further bending cycles. The changes in the gain profiles in the bent and unbent states are moderate, as illustrated by the data given in Fig. 2(c). These variations are much larger than those associated with repeated measurement at any given bend configuration within this range. The inset shows the variation in the normalized gain with hundreds of bending cycles, indicating little evidence for fatigue.

Using similar inverters, we fabricated five-stage ring oscillators. Figure 3(a) provides optical images of oscillators on a PI substrate, and an equivalent circuit diagram. The L_c and L_o values of these transistors are 4 and 2.5 μm, respectively. Figure 3(b) shows the measured wave form at a supply voltage V_{DD} of 4 V. This response shows a frequency of 8.1 MHz, corresponding to a stage delay of 12 ns. The frequency stabilized quickly (less than a fraction of a second) after the supply voltage was applied. The operating voltages are much lower than the 20–45 V and 10–15 V reported for ring oscillators fabricated using organic transistors and polycrystalline Si on flexible substrates, respectively,[1–3] as well as the 43 V value reported for systems that use nanowire transistors on rigid glass substrates.[12] Additional improvements in device design, such as reduction of contact overlap and channel length, should lead to significantly higher oscillation frequencies. We performed bending tests on the ring oscillators. Figure 3(c) shows some results that indicate frequencies of 8.1 MHz in the unbent state (red), 8.5 MHz at 0.23% tensile strain (green), and 7.3 MHz at 0.23% compressive strain (blue). The change in the operating frequency with strain might result from slight strain-induced changes in the mobility of the silicon[13] in combination with other variations in different parts of the device. The results, then, indicate that although the devices can operate at reasonably high levels of bending-induced strain, subtle variations in device properties can lead to changes in circuit operation, in this case at the ~10%–20% level for the oscillation frequency. The circuit operation ceases at bending strains that are far below those needed to cause complete failure of the individual transistors or any of the inverters. At the circuit level, even slight mismatches in gain profiles of any of the five stages induced by bending will render the oscillator inoperable. There is, then, a fundamental difference of the failure mechanisms of the transistors or inverters (i.e., cracking or

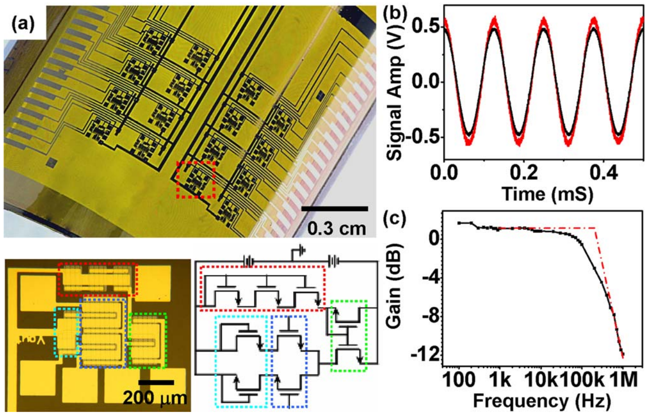

FIG. 4. (Color online) (a) Image of an array of differential amplifiers on a PI substrate (top), magnified view of a single amplifier (bottom left), and circuit diagram (bottom right) [red: current source (three transistors with L_c=30 μm and W=80 μm), green: current mirror (two transistors with L_c=40 μm, W=120 μm and L_c=20 μm, W=120 μm), blue: differential pair (two transistors with L_c=30 μm and W=180 μm), cyan: load (two transistors with L_c=40 μm and W=80 μm)]. The L_o values of these transistors are 15 μm. (b) The time variation of the input and output signals (black: V_{IN} and red: V_{OUT}). (c) Frequency response of a representative differential amplifier with an input signal of 500 mV PP.

delamination of critical material layers) and failure of the ring oscillators (i.e., device property changes sufficient to prevent circuit oscillation). For circuits that must operate in conditions that involve bending, and especially those that require more delicate matching of device properties than the simple ring oscillators described here, these variations should be considered in the mechanical and electrical designs.

In some cases, the circuits do not have to operate during bending, but rather they must be bendable for installation. An example is a structural health monitor, in which the flexible circuit is wrapped around a rigid structure where it remains for monitoring purposes. Differential amplifiers are useful building blocks for such systems. We built such devices using Si NMOSFETs on flexible PI substrates to demonstrate the relevant capability. Figure 4(a) shows an image of a printed array on a PI substrate and its equivalent circuit diagram. This differential amplifier consists of four different components including a current source, current mirror, differential pair, and load. Figures 4(b) and 4(c) show the time variation of the input and output signals and the variation of the differential amplifier gain as a function of the frequency of an input signal with amplitude of 500 amV peak to peak (PP). This differential amplifier exhibits an output voltage gain of ~1.3 for a 500 mV PP input signal in good agreement with the P-SPICE simulations used to design the circuit, and can be operated in a bent configuration. The level of bendability is similar to that for the inverters of Fig. 2, suitable for integration into structural monitors for applications in aerospace.

In conclusion, single-crystalline silicon ribbons generated from wafer scale sources of material provide a high performance printable semiconductor and a relatively easy, printing-based path to transistors and integrated circuits on flexible plastic substrates. Our preliminary results suggest that individual devices of this kind can be integrated into complex circuits with functionalities appropriate for diverse applications. Depending on the requirements of these applications, variations in circuit operation induced by bending strains must be considered in the electrical and/or mechanical aspects of device/circuit design.

This work was supported by the Department of Energy (DEFG02-91ER45439) and used the Center for Microanalysis of Materials of the Frederick Seitz Materials Research Laboratory supported by the Department of Energy (DEFG02-91ER45439). Work in developing the differential amplifiers was partially supported by NextGen Aeronautics under Department of Defense Small Business Research Innovation Program (W31P4Q-05–C0308).

[1]N. Stingelin-Stutzmann, E. Smits, H. Wondergem, C. Tanase, P. Blom, P. Smith, and D. De Leeuw, Nat. Mater. **4**, 601 (2005).
[2]M. G. Kane, L. Goodman, A. H. Firester, P. C. van der Wilt, A. B. Limanov, and J. S. Im, Tech. Dig. - Int. Electron Devices Meet. **2005**, 1087.
[3]T. Afentakis, M. Hatalis, A. T. Voutsas, and J. Hartzell, IEEE Trans. Electron Devices **27**, 460 (2006).
[4]P. F. Carcia, R. S. McLean, M. H. Reilly, and G. Nunes, Jr., Appl. Phys. Lett. **82**, 1117 (2003).
[5]S.-H. Hur, D.-Y. Khang, C. Kocabas, and J. A. Rogers, Appl. Phys. Lett. **85**, 5730 (2004).
[6]M. C. McAlpine, R. S. Friedman, S. Jin, K. Lin, W. U. Wang, and C. M. Lieber, Nano Lett. **3**, 1531 (2003).
[7]E. Menard, K. J. Lee, D. Y. Khang, R. G. Nuzzo, and J. A. Rogers, Appl. Phys. Lett. **84**, 5398 (2004).
[8]J.-H. Ahn, H.-S. Kim, K. J. Lee, Z.-T. Zhu, E. Menard, R. G. Nuzzo, and J. A. Rogers, IEEE Electron Device Lett. **27**, 460 (2006).
[9]H.-C. Yuan and Z. Ma, Appl. Phys. Lett. **89**, 212105 (2006).
[10]S. Mack, M. Meitl, A. Baca, Z.-T. Zhu, and J. A. Rogers, Appl. Phys. Lett. **88**, 213101 (2006).
[11]S.-M. Han, M.-Y. Shin, J.-H. Park, and M.-K. Han, J. Non-Cryst. Solids **352**, 1434 (2006).
[12]R. S. Friedman, M. C. McAlpine, D. S. Ricketts, D. Ham, and C. M. Lieber, Nature (London) **434**, 1085 (2005).
[13]F. Yuan, C.-F. Huang, M.-H. Yu, and C. W. Liu, IEEE Trans. Electron Devices **53**, 724 (2006).